28 GHz Propagation Channel Measurements for 5G Microcellular Environments

C. Umit Bas*, Rui Wang*, Seun Sangodoyin*, Sooyoung Hur†, Kuyeon Whang†,
Jeongho Park†, Jianzhong Zhang‡, and Andreas F. Molisch*
*University of Southern California, Los Angeles, CA, USA
†Samsung Electronics, Suwon, Korea
‡Samsung Research America, Richardson, TX, USA

***Abstract*—This paper presents results from several 28 GHz propagation channel measurement campaigns performed with a real-time channel sounder that is capable of performing directionally-resolved channel measurements in dynamic environments. We summarize the key results from three measurement campaigns; microcellular in a residential environment, stationarity region, and dynamic scatterers measurements in urban environments.**

I. Introduction

The design and deployment of any wireless system require a thorough understanding of the wireless propagation channel. Specifically for millimeter-wave (mm-wave) frequencies, due to the higher path- and penetration losses, any system operating over distances larger than a few meters will have to utilize beamforming antenna arrays [1], [2]. The statistics of the angular spectrum and their temporal variations should be taken into account when designing a system with such beamforming capabilities. However, almost all of the directional outdoor measurements for mm-wave frequencies were performed with rotating horn antenna channel sounders, which can not measure in real-time and thus are not suitable for dynamic channels [3].

In this paper, we summarize results from our recent channel sounding campaigns performed with a double-directional real-time mm-wave channel sounder [4], [5] which is described in Section II. Section III summarizes the results obtained in three measurement campaigns performed to investigate the different aspects of the microcellular environment at $28\,\mathrm{GHz}$.

II. Measurement Setup

The channel sounder used in these measurements is a real-time mm-wave channel sounder [4], [5]. By using beamforming arrays, it can perform 90° sweeps in the azimuth at the receiver (RX) and the transmitter (TX). Furthermore, TX and RX are synchronized by using GPS-disciplined Rubidium frequency references without requiring a physical connection.

Table I. Sounder Parameters Used in Measurements

Parameters	**Microcell [6]**	**Stationarity [7]**	**Dynamic [8]**
Frequency	27.85 GHz		
Bandwidth	400 MHz		
Array size	8 by 2		
Beam steering	-45° to 45°		
3dB beam width	12°		
Steering steps	5°		10°
Switching speed	$2\mu s$		
TX EIRP	57 dBm		
RX noise figure	$\leq$ 5 dB		
SISO duration	2 μs		
SISO repetition	10	10	1
Total sweep time	14.44 ms	14.44ms	0.4 ms

Thanks to the flexible design, the operation parameters of the channel sounder can be modified on a per campaign basis. Table I summarizes the parameters used in the three measurement campaigns. For the residential microcell and stationarity region measurements, we employed waveform repetition to improve RX signal to noise ratio by averaging. For the dynamic measurements, we only measured a subset of available azimuth beams to increase the snapshot repetition frequency to measure higher Doppler frequencies.

III. Measurement Campaigns

A. Residential Microcell

In [6], we investigated path-loss (PL) and delay spread in a suburban residential environment for a microcell and the impact that beamforming has on it. The obtained results also include the effects of the foliage, which is typical to a suburban street. The measurements were taken in two scenarios; first when the RX is on the same street with the TX (denoted as line-of-sight (LoS), although most of the time the direct path was blocked by foliage), and when the RX is on a crossing street and the direct path is blocked by buildings.

The estimated parameters for the PL model are summarized in Table II. The directional PL is calculated by using the power of the best TX-RX beam pair as the received power, while for the omnidirectional PL, we combine the power received via all TX-RX beams. The TX-RX distances for LoS measurements vary from $36\,\mathrm{m}$ to $400\,\mathrm{m}$, and from $130\,\mathrm{m}$ to $273\,\mathrm{m}$ for the non-LoS (NLoS). Hence the provided PL model is only applicable within these ranges. Furthermore, the median root mean square delay spreads (RMS-DS) for the omnidirectional power delay profiles were estimated as $25.63\,\mathrm{ns}$ and $67.18\,\mathrm{ns}$ for LoS and NLoS respectively.

B. Dynamic Environment

In [8], we presented the first dynamic double directional measurements for a microcell scenario. A sample measurement location is shown in Fig. 1. During this measurement, both the

Table II. Parameters of the Path Loss Models

	Data	n	P_0	$\chi\sigma$	
				σ	P-Value
Omni	LoS - ABG Model	2.82	63.47	6.44	0.975
	LoS- CI Model	2.92	61.34	6.45	0.978
	NLoS - ABG Model	4.97	29.53	2.58	0.745
	NLoS - CI Model	3.58	61.34	3.06	0.706
Directional	LoS - ABG Model	3.17	58.01	7.75	0.840
	LoS - CI Model	3.15	61.34	7.76	0.928
	NLoS - ABG Model	5.85	18.12	4.53	0.856
	NLoS - CI Model	3.96	61.34	5.06	0.958

Submitted On: September 29, 2018
Accepted On: October 1, 2018

Fig. 1. Environment for dynamic measurements.

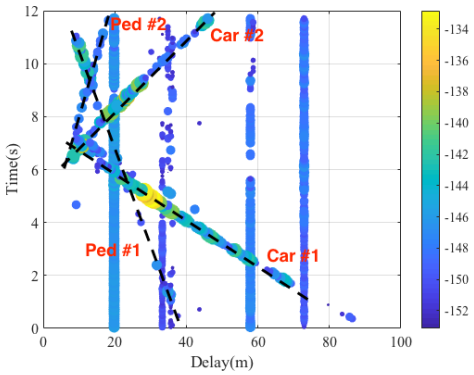

Fig. 2. Temporal evolution of the power delay profile (dB).

RX and TX are placed parallel to the road facing the same direction and perform 90° scans in the azimuth. The TX is placed at $4\,\mathrm{m}$ height, while the RX is at $1.8\,\mathrm{m}$. Along with some fixed objects, there are four moving objects; two cars and two pedestrians as indicated in Fig. 1.

Fig. 2 shows the power of the multipath components and their evolution over time. The multipath components for the four moving objects are clearly visible and their routes are marked in Fig. 2.

C. Stationarity Region

In a third campaign, we investigated the stationarity region of MIMO mm-wave channels at 28 GHz based on an outdoor measurement campaign. We analyzed results in an urban microcell LoS and LoS to NLoS transition region scenario, for the stationarity region of shadowing, power delay profile and the angular power spectrum [7].

We have found that the foliage effect can significantly alter the PL exponent even in the LoS scenario. For our measurements, this effect resulted in the proposed dual-slope PL model in Fig. 3. The propagation loss increases rapidly, about 30 dB, during the transition from LoS to NLoS. We propose to model it with a street-by-street PL model, similar to the method in [9]. More results related to the PL fitting can be found in Fig. 3. The autocorrelation distance of shadowing is 1.2 m in the LoS route, although this value might be affected by the signal variation observed in the two-path channel. It increases up to $4.8\,\mathrm{m}$ for the LoS to NLoS transition route. The average correlation distance as computed based on the similarity of the power delay profiles, is $0.9\,\mathrm{m}$ for the LoS route. It can become as high as $4\,\mathrm{m}$ at the beginning section of the transition route and drops to about $1.26\,\mathrm{m}$ afterward. The analysis based on the correlation of shadowing and PDP has suggested that mm-wave channels exhibit a smaller stationarity region compared with cm-wave channels.

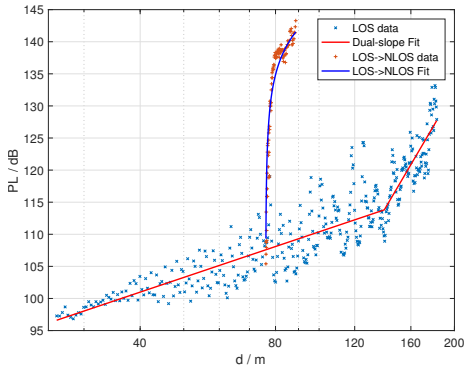

Fig. 3. The path-loss data fitting for the microcell LoS and LoS to NLoS transition region scenarios.

IV. Conclusions

This paper discusses results from various 28 GHz propagation channel measurements performed with a real-time double-directional channel sounder for three different investigations. Through extensive measurements allowed by the nature of the used channel sounder, we were able to propose statistical models for path-loss, shadowing, RMS-DS and the stationarity region. Furthermore, we presented results from the first dynamic double directional measurement campaign for microcell environment at mm-wave frequencies.

Acknowledgements

Part of this work was supported by grants from the National Science Foundation (grants CIF-1618078, CNS-1457340, ECCS-1126732) and National Institute of Standards and Technology (grant 60NANB17D317).

References

[1] F. Boccardi, R. W. Heath, A. Lozano, T. L. Marzetta, and P. Popovski, "Five disruptive technology directions for 5G," in IEEE Communications Magazine, vol. 52, no. 2, pp. 74–80, February 2014.

[2] A. F. Molisch, A. Karttunen, R. Wang, C. U. Bas, S. Hur, J. Park, and J. Zhang, "Millimeter-wave channels in urban environments," in 2016 10th European Conference on Antennas and Propagation (EuCAP), April 2016, pp. 1–5.

[3] T. S. Rappaport, G. R. Maccartney, M. K. Samimi, and S. Sun, "Wideband millimeter-wave propagation measurements and channel models for future wireless communication system design," in IEEE Transactions on Communications, vol. 63, no. 9, pp. 3029–3056, September 2015.

[4] C. U. Bas, R. Wang, D. Psychoudakis, T. Henige, R. Monroe, J. Park, J. Zhang, and A. F. Molisch, "A real-time millimeter-wave phased array MIMO channel sounder," in 2017 IEEE 86th Vehicular Technology Conference (VTC-Fall), September 2017, pp. 1–6.

[5] C. U. Bas, R. Wang, S. Sangodoyin, D. Psychoudakis, T. Henige, R. Monroe, J. Park, J. Zhang, and A. F. Molisch, "Real-time millimeter-wave MIMO channel sounder for dynamic directional measurements," arXiv preprint arXiv:1807.11921, 2018.

[6] C. U. Bas, R. Wang, S. Sangodoyin, S. Hur, K. Whang, J. Park, J. Zhang, and A. F. Molisch, "28 GHz microcell measurement campaign for residential environment," in 2017 IEEE Global Communications Conference (GLOBECOM), December 2017, pp. 1–6.

[7] R. Wang, C. U. Bas, S. Sangodoyin, S. Hur, J. Park, J. Zhang, and A. F. Molisch, "Stationarity region of mm-wave channel based on outdoor microcellular measurements at 28 GHz," in 2017 IEEE Military Communications Conference (MILCOM), October 2017, pp. 782–787.

[8] C. U. Bas, R. Wang, S. Sangodoyin, S. Hur, K. Whang, J. Park, J. Zhang, and A. Molisch, "Dynamic double directional propagation channel measurements at 28 GHz-Invited paper," in 2018 IEEE 87th Vehicular Technology Conference (VTC Spring), June 2018, pp. 1–6.

[9] A. F. Molisch, A. Karttunen, S. Hur, J. Park, and J. Zhang, "Spatially consistent pathloss modeling for millimeter-wave channels in urban environments," in 2016 10th European Conference on Antennas and Propagation (EuCAP), April 2016, pp. 1–5.